

Self-assembly of oxide-supported metal clusters into ring-like structures

Kristoffer Meinander,* Kai Nordlund, and Juhani Keinonen

Department of Physics, University of Helsinki,

P.O. Box 43, FI-00014 Helsinki, Finland

Abstract

Self-assembly is a phenomenon that continuously occurs at the nanoscale, as atoms form pre-determined building blocks, such as molecules and clusters, which then themselves gather into structures of a larger scale. The interplay of competing forces is a decisive factor in the emergence of these organized systems, but the precise mechanism, with which this self-assembly progresses, is seldom known. Using a combination of physical cluster deposition and atomic force microscopy, we have investigated the spontaneous formation of μm -sized rings of SiO_x -supported metal nanoclusters. With the help of molecular dynamics simulations, we show that the competition between short-range van der Waals attractions and long-range repulsive dipolar forces, induced by the ionic surface, plays a key role in the self-assembly of these structures.

I. INTRODUCTION

The physical basis for self-assembly of complex nanostructures usually lies in the balance between weak long-range van der Waals or dipole interactions and strong short-range covalent, metallic, or ionic interactions¹⁻³. E.g., self-assembly of block co-polymer structures relies on different types of polymers that bind to each other with covalent bonds at one end, while the nanostructure is formed by the repulsive long-range interactions of the other ends⁴⁻⁶. Another example is the self-assembly of thiol polymer chains on gold, which relies on a balance of sulfur-metal bonding that binds the organic molecules to gold and long-range interactions between the polymers that drive them to an ordered configuration⁷. It is therefore crucial to understand the balance of short- and long-range interactions to enable controlled design of increasingly complex nanostructures. However, even in some of the prototypical systems, e.g. thiol on gold, the interactions have proven to be surprisingly complex and are still not fully understood⁸⁻¹⁰.

Here we examine one of the (in principle) simplest systems in nanoscience, namely that of metal nanoclusters deposited on silica. Despite its simplicity, even this system exhibits a surprisingly complex behavior¹¹⁻¹³. The interactions between metallic clusters and their supporting surfaces can have interesting implications for both thin film growth techniques and especially catalyst technologies^{14,15}, where a controlled deposition of particles is of the utmost importance. This controllability is, however, highly jeopardized, as the magnitudes of many of the physical properties of nanoclusters, such as polarizability^{11,13,16} and surface diffusion^{12,17,18}, vastly exceed classical predictions, due to effects of their nanoscale size. The self-assembly of dispersions of particles has previously been observed for colloidal suspensions of magnetic nanoparticles¹⁹⁻²¹ and highly polar particles in solution²², as well as nano- and micro-scale particles in evaporating drops of particle-containing solvents^{23,24}. These have all been guided by external forces, such as magnetic fields or the flow of solvents, but little interest has been focused on effects induced by the supporting surface.

Using a combination of experiments, in which metallic nanoclusters were deposited onto the native oxide layer of Si(111) single crystal substrates, and mesoscale molecular dynamics (MD) simulations, we show that metal clusters can spontaneously form μm -sized rings on the surface. Based on our results, we propose that this formation can be explained by a balance of long-range, surface induced, repulsive dipolar interactions and short-range attractive van

der Waals forces between individual clusters. We also determine the time dependence of the self-assembly, showing that it undergoes several distinct stages on macroscopic time scales.

II. METHODS

A. Cluster deposition and AFM imaging

In order to study the influence of ionic, polarizable, surfaces, such as silica, on metallic clusters, we deposited nanoclusters, with average diameters of 5.0 ± 0.1 nm, onto Si(111) single crystal substrates, which were covered with a native oxide layer, SiO_x . After deposition, sample surfaces were imaged by atomic force microscopy (AFM) in ambient conditions. Deposition of both copper and iron clusters, two transition metals with different chemical and magnetic properties, but similar static polarizabilities^{25,26}, was performed on separate samples, in order to rule out material-dependent effects.

Clusters were produced in a condensation cell-type cluster source (NC200U, Oxford Applied Research, Oxfordshire, UK), where the solid material is sputtered by a magnetron discharge and swept by a viscous stream of argon gas into the condensation chamber, where it cools down to room temperature²⁷. The supersaturated metal atoms aggregate and are then carried further, by the argon flow, through several differential pumping stages, during which most of the carrier gas is pumped away, entering the deposition chamber as a molecular beam of clusters. The pressure was 1.0×10^{-3} mbar in the condensation chamber and better than 1.0×10^{-8} mbar in the deposition chamber during operation.

Deposition onto the SiO_x covered Si(111) substrates was carried out at low fluxes, $< 10^7$ clusters/cm²s, for a deposition time of approximately 5 hours for each sample. Prior to loading into the deposition chamber, the Si(111) substrates were cleaned in a sulfoperoxide mixture ($\text{H}_2\text{SO}_4:\text{H}_2\text{O}_2$) and then rinsed in deionized water. **An annealing of the substrate to 200 °C in vacuum prior to deposition of the clusters did not change any results.** Deposition with both copper and iron clusters was carried out separately.

After deposition, samples were kept in vacuum for up to 24 hours, after which they were removed from the deposition chamber and studied by atomic force microscopy, using an Autoprobe CP Research AFM (ThermoMicroscopes, Sunnyvale, CA, USA), operated in intermittent-contact (tapping) mode. All AFM measurements were conducted under am-

bient conditions using MikroMasch NSC11 triangular Si cantilevers coated with Si_3N_4 ($k = 42 \text{ N/m}$), with typical end-radii $< 10 \text{ nm}$ and cone angles $< 30^\circ$ for the probe tips. Intermittent-contact mode was used in order to maximize image resolution, without unintentionally subjecting the samples to lateral forces during the measurements. All AFM images were processed using the image processing software of the AFM system.

Cluster mass distributions were measured with a built-in quadrupole mass spectrometer connected to the deposition system, and cluster size distributions were determined through subsequent AFM measurements. The shape of each distribution was consistent for both measurement techniques. The average heights (\approx diameters, for spherical clusters) of $5.0 \pm 0.1 \text{ nm}$, indicated here, are those measured with AFM, where the error is the standard deviation of the cluster sizes.

B. Molecular dynamics simulations

Ring formation was simulated, using classical molecular dynamics methods, with a code specifically developed for this system. Clusters were treated as single entities with a size and mass corresponding to the 5 nm in diameter clusters of the experiment. The cluster-cluster interactions were modeled with a potential that was built up using analytical models for the dipole-dipole interaction²⁸

$$U_{d-d} = \frac{p^2}{4\pi\epsilon_0 r^3}, \quad (1)$$

where p is the strength of the cluster dipole and r is the distance between the clusters, and a Lennard-Jones potential²⁹

$$U_{vdW} = \epsilon \left[\left(\frac{\sigma}{r} \right)^{12} - 2 \left(\frac{\sigma}{r} \right)^6 \right], \quad (2)$$

where ϵ is the strength of the interaction, σ the equilibrium distance and r the distance between the clusters, for the van der Waals interactions. A velocity dependent frictional force was also added, in order to allow for limited surface diffusion velocities, resulting in a total potential of

$$U_{tot} = U_{d-d} + U_{vdW} + U_{friction}. \quad (3)$$

The two parameters that had the most effect on simulation results were the dipole strength, p , and the strength of the van der Waals interaction, ϵ . Several combinations of these parameters were tested, from which it was concluded that values giving similar

magnitudes for the strengths of the dipolar and van der Waals interactions, when $p \approx 10^{-27}$ Cm and $\varepsilon \approx 2$ eV, gave results comparable to the experiments. This seems reasonable, as both interactions stem from variations in the electronic distributions of the clusters. Similar ratios between these two parameters resulted in similar cluster configurations, whereas different absolute values, at the same ratios, only affected the speed at which cluster movement took place.

The given values of p and ε are several orders of magnitude higher than what would be experimentally expected, although their ratio is within an order of magnitude comparable to this³⁰, due to a limit in achievable simulation times. The time-step for the simulations could be as large as 5 ps, due to the heavy mass of the clusters, but was nonetheless too small for the time-scales of the experiments to be attainable. In order to speed up the movement of the clusters, however, interaction strengths were exaggerated and frictional forces were set as very low. Simulation times of up to 1 μ s were achieved, which was sufficient for the formation of rings from initially random distributions of clusters. With lower values of p and ε , rings are expected to form at longer time-scales, approaching those of the experiments.

The equilibrium distance was chosen such that the optimal situation occurred when two clusters were barely touching, i.e., $\sigma = 5.0$ nm. Cluster densities between 1 – 1000 clusters/ μ m² were tested. The longest time-scale effects of the experimental results, the formation of large cluster aggregates, were obtained through simulations, when the strength of the van der Waals interaction was set as much larger than the dipole strength. This corresponded to the experimentally observed situation, where surface induced dipoles have diminished due to oxidation of the clusters.

III. RESULTS AND DISCUSSION

For the case of experimental cluster deposition, samples exhibited two different types of features that could be related to either a short time-scale interaction or a long time-scale interaction. Short time-scale features were present on the surfaces immediately after deposition and up to 30 hours after introduction into the ambient, whereas long time-scale features only appeared once samples had been left in the ambient for more than four days.

A. Short time-scale effects

Typical images of the sample surfaces, directly after deposition and introduction into the ambient, are shown in Fig. 1, where a self-assembly of the individual clusters into ring-like structures can clearly be seen, for different cases of low surface coverage (Fig. 1(a)-(c)) and higher coverage (Fig. 1(d)-(e)). Depending on the areal density of the supported clusters, either rings, at low coverage, or circular areas depleted of clusters, at high coverage, were formed. The typical diameters of these rings or circular areas ranged from $\sim 1 \mu\text{m}$ up to $\sim 5 \mu\text{m}$. Larger aggregates of clusters, with heights clearly surpassing those of single clusters, were observed, pointing toward the simultaneous aggregation of clusters into massive islands. Similar results were observed for clusters of both copper and iron.

The fact that the clusters are clearly visible as independent objects, an effect which is the same for two different metals, shows that the metallic cohesion within each individual cluster is sufficiently high for clusters of this size to keep them intact, while an explanation of the self-assembly must be sought from weaker dipolar or van der Waals forces. The ring formation, and aggregation of larger structures, points toward a rapid diffusion of the supported clusters, the occurrence of which has been well established by previous studies^{12,31}, under influence of both long-range and short-range forces, long after the deposition event has taken place. Surface diffusion of the clusters is promoted by a relatively weak metal-SiO_x interaction, an effect which would not present itself with metallic clusters on, e.g., pure Si, as the metal-Si interaction is much stronger³².

The aggregation of clusters into islands and the cohesion between adjacent clusters in each ring is guided by enhanced attractive van der Waals interactions of nanoscale metal clusters^{33,34}, while the long-range interactions are most likely predominantly governed by repulsive forces. One possible explanation for the source of this repulsive interaction is the existence of dipoles in the clusters, induced by the ionic, polar surface. This is supported by the fact that the ionic silica surface can easily induce dipoles, either through a partial transfer of charge to the clusters or due to a local polarity of the surface, perpendicular to the substrate surface, in clusters that have provenly high polarizabilities^{11,13}. The surfaces of single-crystal bulk and thin film polar materials will usually reconstruct in order to cancel the electrostatic instability, caused by the build-up of a macroscopic dipole moment from the small non-zero dipole of each layer of material³⁵. A small dipole moment may, however, still

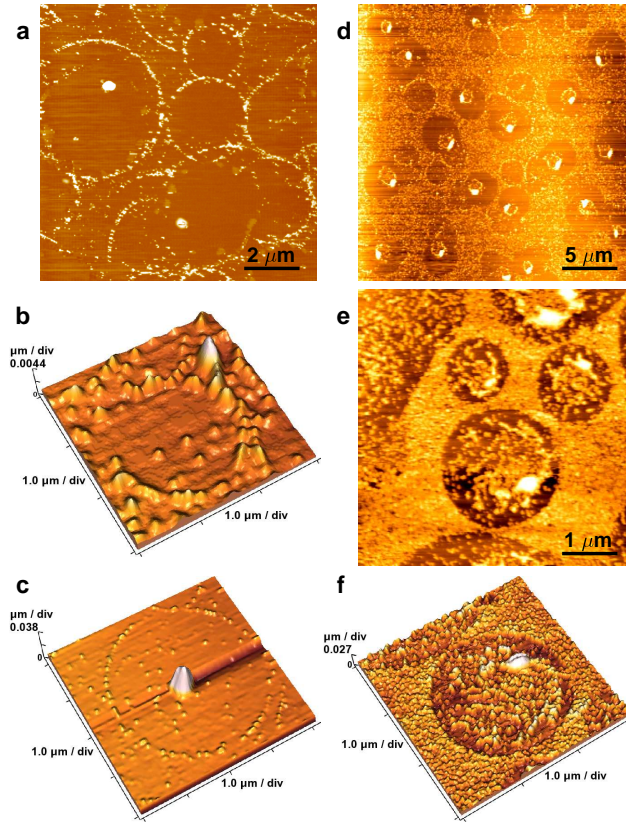


FIG. 1: AFM images of supported metal cluster configurations. (a) A region of low cluster coverage, showing several ring-like structures. (b) A cluster-ring with a nearly depleted center, and (c) a ring with a large aggregate at its center, both found in areas of low cluster coverage. (d) A region of slightly higher cluster coverage, where smaller rings have formed inside of depleted areas, as inter-cluster distances are short enough for van der Waals forces to be dominant. At even higher coverage, in (e) and (f), aggregation is observed inside of circular areas, whereas a stable monolayer coverage remains intact elsewhere. Due to convolution from the AFM tip, lateral features appear much larger than they are in reality, whereas the height scale gives the correct size of the particles. The height scale of the AFM images is depicted by the color scheme, where the lightest areas are the highest and the darkest areas are the lowest.

be sustained at the surface of many materials, which, especially in the case of amorphous materials, such as native SiO_x , can be rather significant.

Directly after deposition of the clusters, competition between these attractive and repulsive forces will decide how the configuration of the clusters on the surface evolves. Clusters that are separated by longer distances will be pushed further from each other, whereas

clusters close to each other will agglomerate. If coverage is high, as in Fig. 1(d)-(f), the interplay of forces will hold the clusters in place in a monolayer matrix on the surface, with the exception of points where clusters are closer to each other and can coalesce into larger islands. During the process of aggregation, these islands will cause the formation of regions that are depleted of clusters. If coverage is lower, exotic structures, such as rings, may be formed.

It should also be noted that Cu and Fe behave very similarly in the experiment, even though these metals interact quite differently with pure silicon³². This gives evidence that the interactions are indeed electrostatic and not covalent by nature.

Previous studies have shown that the adhesion between copper clusters and SiO_x surfaces increases as clusters are fully oxidized³⁶, an event which occurs within 29 hours of extraction from vacuum, for clusters of sizes around 5 nm³⁷. The process of introducing the samples to the ambient, will therefore result in both a slower surface diffusion as well as a lessening of the induced dipoles, as clusters lose their metallic properties. The existence of small clusters, of below-average size, within some of the ring-like structures (in areas that are otherwise void of large cluster populations), can be explained by a faster oxidation, and therein a faster immobilization, of these smaller clusters. The seemingly random positions of the larger cluster aggregates as compared to individual clusters, is a result of the lower diffusion rate for the much more massive islands.

In order to better understand the formation of these ring-like structures, we performed MD simulations, where the interaction between clusters was guided by a potential that combined both long-range dipolar repulsive forces and short-range van der Waals interactions. The main purpose of the simulations was to construct a minimal model displaying results similar to the experimental results. Although somewhat dissimilar, and often complex, interaction models can produce comparable behavior when used in MD, our goal was to create one of the simplest possible models that could correctly portray the experimental self-assembly of our metal nanoclusters. The functional form of our potential, and its main components, is given in Fig. 2. The results of these simulations indicate that the self-assembly of metallic nanoclusters into ring-like structures can occur as a direct consequence of the interaction between cluster dipoles that are induced by the ionic silica surface.

As previously mentioned in Section II B, it was necessary to keep the ratio between the dipole strength, p , and the strength of the van der Waals interaction, ε , fairly constant

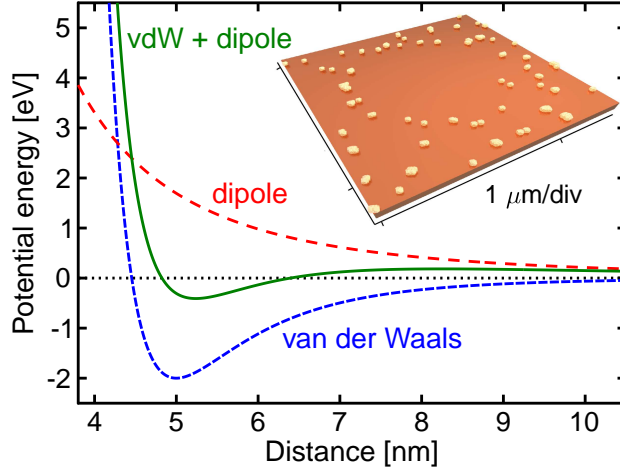


FIG. 2: The potential function used for modeling cluster-cluster interactions, built up from a van der Waals (vdW) component and a dipole-dipole interaction. Essentially the strength of the dipolar interaction, depending on the surface properties and the oxidation of the clusters, determines the distance after which clusters are no longer attracted, i.e., where the gradient of the potential energy curve is zero, at ~ 8 nm. Variations in the dipole strength will cause this distance to either grow, for stronger dipoles, or shrink, for weaker dipoles, an effect which will determine the size of the ring-like structures. The inset shows a **simulated ring configuration**, which has appeared during the relaxation of an initially random cluster distribution, with roughly the same size as cluster-rings seen experimentally.

throughout the simulations. Increased values of p , without similar increases in ε , caused the formation of a uniformly dispersed matrix of clusters, as their repulsive interaction was too strong to overcome, whereas the opposite change in the values resulted in the rapid aggregation of all of the clusters. One curious feature that could also be noticed was that ring formation was not readily observed for an initially even distribution of clusters, until small variations in the polarity of the surface were introduced. The deviations in surface polarity, necessary for ring formation, were included in the dipolar contribution of the interaction potential, by introducing randomly distributed perturbations, coupled to specific surface locations, in p . The values of the perturbations were randomly chosen, with a maximum value of $\Delta p \sim 0.05 \times p$. The inclusion of these random perturbations is validated by the fact that small variations in the induced dipoles of SiO_x supported clusters would also be experimentally expected, as the deviations in the strength of surface dipoles on the

amorphous surface are necessarily present.

A cluster configuration resulting from the simulations is shown in the inset in Fig. 2, where a clear ring-like structure, very similar to that of the AFM results in Fig. 1(b), is evident. Areas of the surface that had a higher polarity, were more likely to be depleted of clusters, as compared to areas causing a lesser polarization. Variations in the strength of p could mainly be observed to result in a change in the resulting size of the ring-like structures.

In order to test whether such variations in surface polarity or rather the polarity of individual clusters had the greatest effect on cluster interactions, a sample onto which clusters were deposited consecutively on two separate occasions, with a latent period of 10 hours (in vacuum) in between, was experimentally prepared. Fig. 3 shows an AFM image of the surface of this sample, from which it can be seen that concentric rings have formed in most places where rings occur. This suggests that it is indeed the variations in polarity of specific spots on the surface that induce the ring formation, and not a difference resulting from size or oxidation level of the clusters.

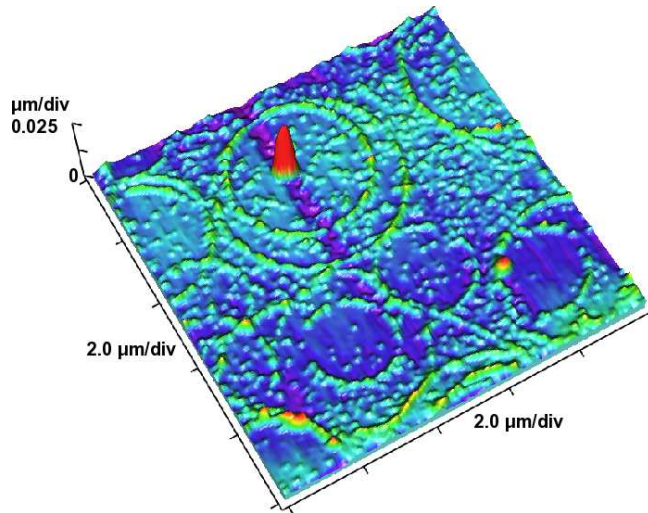


FIG. 3: An AFM image of a surface onto which clusters have been deposited on two separate occasions. The cluster covered surface was allowed to stabilize in vacuum for approximately 10 hours between each deposition, which was sufficient time for the formation of the first set of rings. The appearance of concentric rings hints toward the role of specific points on the surface in arrangement of the deposited clusters.

B. Long time-scale effects

Further evidence of the diffusion of clusters, even after oxidation, can be seen in Fig. 4, where AFM images of the sample surfaces, taken several days after the deposition event, are shown. As the clusters are fully oxidized, after introduction to the atmosphere, the repulsive dipolar forces have disappeared, and only van der Waals interactions remain, guiding clusters toward aggregation. Fig. 4(a)-(b) show the progress of this aggregation of clusters into cluster islands, one week and two weeks, respectively, after the actual deposition has occurred. After two weeks of diffusion, a uniform matrix of cluster islands, clearly visible by optical microscopy at a magnification of $\times 1000$ (Fig. 4(c)), has covered the sample surface. Evidence of similar migration and agglomeration of copper clusters has previously been observed³¹.

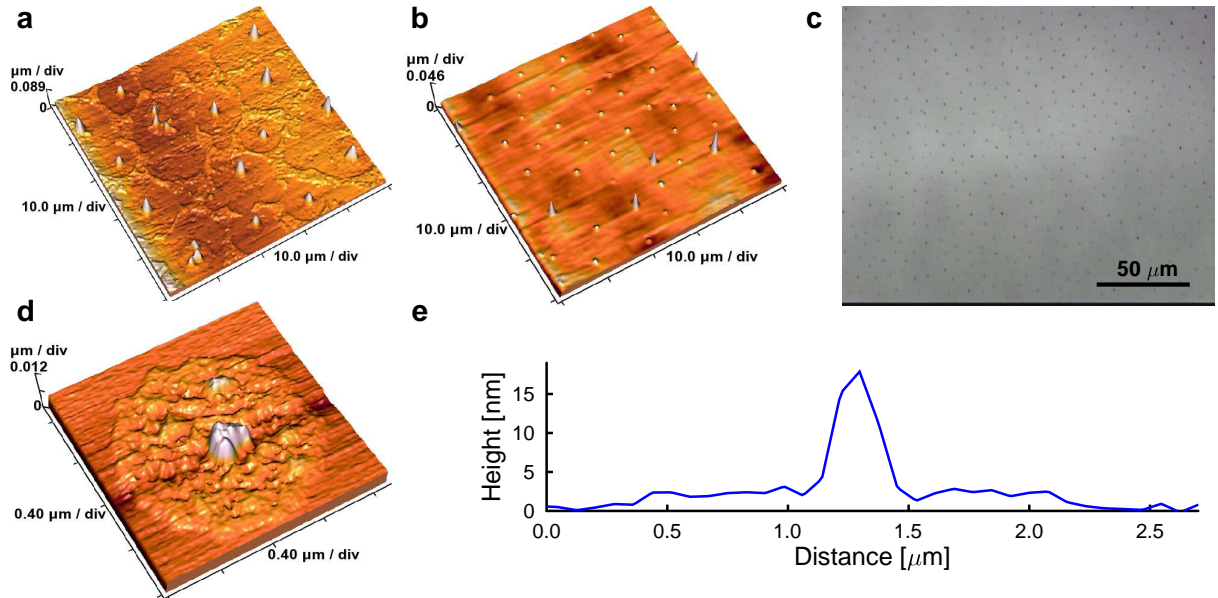


FIG. 4: AFM images of the surfaces were also acquired (a) one week after deposition and (b) two weeks after deposition. In the latter image all clusters have coalesced into aggregates, forming a matrix of dots that is clearly visible even in (c) an optical micrograph of the surface. An AFM image with a larger magnification of an aggregate is shown in (d) and the height profile, through the center of a similar aggregate is given in (e), revealing how the center peak is much higher than the diameter of a single cluster, whereas the surrounding halo has a height of only a few nm, much lower than the original clusters.

A higher magnification of a single cluster island (Fig. 4(d)) shows a larger central island surrounded by a halo of smaller particles. The height profile through the cross-section of a similar island (Fig. 4(e)) shows that these smaller particles are in fact lower than the original height of the nanoclusters, suggesting that the clusters are gradually being flattened out³⁸, or even that copper is diffusing into the silica substrate.

These long time-scale effects could possibly be avoided, or at least postponed, by either leaving the samples in vacuum, or by embedding the clusters in some sort of encapsulating material, thereby increasing the usefulness of these self-assembled structures in any future applications.

IV. CONCLUSION

In conclusion, we have experimentally observed the formation of ring-like structures of metallic nanoclusters supported on silica surfaces. Using molecular dynamics simulations, we have shown that this can be explained by the competition between isotropic van der Waals interactions and repulsive dipolar forces, which are induced by the ionic substrate. Slight variations in the polarity of the surface are a prerequisite for the formation of ring-like structures.

An increase of the dipolar forces results in an increase in size of the cluster rings, whereas oxidation of the clusters will diminish the surface-induced dipoles, leading to more aggregation. This understanding of the balance of different kinds of short-range and long-range forces paves the way for the design of new deposition methods and conditions to form new classes of metal-based self-assembled nanostructures.

Acknowledgements

This work was performed within the Finnish Centre of Excellence in Computational Molecular Science (CMS), financed by The Academy of Finland and the University of Helsinki. We also gratefully acknowledge financial support from the Magnus Ehrnrooth

- * Electronic address: kristoffer.meinander@gmail.com
- ¹ Hornyak, G. L., Tibbals, H., and J. Dutta, A. R. *Introduction to Nanoscience*. CRC, USA (2008).
- ² C. Niemeyer and C. Mirkin (eds) *Nanobiotechnology*. Wiley-VCH Verlag, Weinheim, Germany (2004).
- ³ Lehn, J. M. *Science* **295**, 2400–2403 (2002).
- ⁴ P. Alexandridis and B. Lindman *Amphiphilic Block Copolymers: Self-Assembly and Applications*. Elsevier, Amsterdam (2000).
- ⁵ Blanazs, A., Armes, S. P., and Ryan, A. J. *Macromol. Rapid Commun.* **30**, 267–277 (2009).
- ⁶ Deming, T. J. *Nature* **390**, 386–389 (1997).
- ⁷ Love, J. C., Estroff, L. A., Kriebel, J. K., Nuzzo, R. G., and Whitesides, G. M. *Chem. Rev.* **105**, 1103–1170 (2005).
- ⁸ Yu, M., Bovet, N., Satterley, C. J., Bengió, S., Lovelock, K. R. J., Milligan, P. K., Jones, R. G., Woodruff, D. P., and Dhanak, V. *Phys. Rev. Lett.* **97**, 166102 (2006).
- ⁹ Maksymovych, P., Sorescu, D. C., and Yates, J. T. *Phys. Rev. Lett.* **97**, 146103 (2006).
- ¹⁰ Grönbeck, H., Häkkinen, H., and Whetten, R. L. *J. Phys. Chem. C* **112**, 15940–15942 (2008).
- ¹¹ Kresin, V. V. and Guet, C. *Phil. Mag. B* **79**(9), 1401–1411 (1999).
- ¹² Deltour, P., Barrat, J.-L., and Jensen, P. *Phys. Rev. Lett.* **78**(24), 4597–4600 Jun (1997).
- ¹³ Knickelbein, M. B. *J. Chem. Phys.* **120**(22), 10450 (2004).
- ¹⁴ Min, B. K., Santra, A. K., and Goodman, D. W. *Catal. Today* **85**, 113–124 (2003).
- ¹⁵ Jensen, P. *Rev. Mod. Phys.* **71**(5), 1695–1735 (1999).
- ¹⁶ Knight, W. D., Clemenger, K., de Heer, W. A., and Saunders, W. A. *Phys. Rev. B* **31**(4), 2539–2540 Feb (1985).
- ¹⁷ Bardotti, L., Jensen, P., Hoareau, A., Treilleux, M., and Cabaud, B. *Phys. Rev. Lett.* **74**(23), 4694–4697 Jun (1995).
- ¹⁸ Bardotti, L., Jensen, P., Hoareau, A., Treilleux, M., Cabaud, B., Perez, A., and Aires, F. C. S. *Surf. Sci.* **367**, 276–292 (1996).
- ¹⁹ Lalatonne, Y., Richardi, J., and Pileni, M. P. *Nature Mater.* **3**, 121–125 (2004).

- ²⁰ Shafi, K. V. P. M., Felner, I., Mastai, Y., and Gedanken, A. *J. Phys. Chem. B* **103**(17), 3358–3360 (1999).
- ²¹ Grzybowski, B. A., Wiles, J. A., and Whitesides, G. M. *Phys. Rev. Lett.* **90**(8), 083903 Feb (2003).
- ²² Tang, Z., Kotov, N. A., and Giersig, M. *Science* **297**, 237–240 (2002).
- ²³ Ohara, P. C., Heath, J. R., and Gelbart, W. M. *Angew. Chem. Int. Ed. Engl.* **36**(10), 1077–1080 (1997).
- ²⁴ Deegan, R. D., Bakajin, O., Dupont, T. F., Huber, G., Nagel, S. R., and Witten, T. A. *Nature* **389**, 827–829 (1997).
- ²⁵ Calaminici, P., Köster, A. M., Vela, A., and Jug, K. *J. Chem. Phys.* **113**(6), 2199 (2000).
- ²⁶ Calaminici, P. *Chem. Phys. Lett.* **387**(6), 253–257 (2004).
- ²⁷ Haberland, H., Insepov, Z., Karrais, M., Mall, M., Moseler, M., and Thurner, Y. *Nucl. Instr. and Meth. in Phys. Res. B* **80/81**, 1320–1323 (1993).
- ²⁸ Jackson, J. D. *Classical Electrodynamics*. John Wiley and sons, Inc., New York, 3 edition (1998).
- ²⁹ Lennard-Jones, J. E. *Proc. Roy. Soc. London Ser. A* **106**(738), 463–477 (1924).
- ³⁰ Pacheco, J. M. and Ekardt, W. *Phys. Rev. Lett.* **68**, 3694 (1992).
- ³¹ Williams, F. J., Malikova, N., and Lambert, R. M. *Catal. Lett.* **90**(3-4), 177–180 (2003).
- ³² Weber, E. R. *Appl. Phys. A* **30**, 1–22 (1983).
- ³³ Serra, L. and Garcias, F. *Phys. Rev. B* **53**(11), 7006–7009 (1996).
- ³⁴ Sonnenberg, J.-P. and Schmidt, E. *Part. Part. Syst. Charact.* **22**, 45–51 (2005).
- ³⁵ Noguera, C. *J. Phys.: Condens. Matter* **12**, R367–R410 (2000).
- ³⁶ Sørensen, A. H., Kühle, A., Hansen, L. T., Busch, H., Christiansen, L. J., Mikkelsen, J., Herholdt-Rasmussen, N., Mørch, K. A., and Bohr, J. *Z. Phys. D* **40**, 509–512 (1997).
- ³⁷ Urban, J., Sack-Kongehl, H., and Weiss, K. *Z. Phys. D* **36**, 73–83 (1996).
- ³⁸ Frantz, J., Rusanen, M., Nordlund, K., and Koponen, I. T. *J. Phys.: Condens. Matter* **16**, 2995–3003 (2004).